© 2017. Published by The Company of Biologists Ltd | Development (2017) 144, 507-518 doi:10.1242/dev.146969

RESEARCH ARTICLE

Vegfd modulates both angiogenesis and lymphangiogenesis during zebrafish embryonic development

Neil I. Bower[1], Adam J. Vogrin[2], Ludovic Le Guen[1], Huijun Chen[1], Steven A. Stacker[2,3], Marc G. Achen[2,3] and Benjamin M. Hogan[1,*]

ABSTRACT

Vascular endothelial growth factors (VEGFs) control angiogenesis and lymphangiogenesis during development and in pathological conditions. In the zebrafish trunk, Vegfa controls the formation of intersegmental arteries by primary angiogenesis and Vegfc is essential for secondary angiogenesis, giving rise to veins and lymphatics. Vegfd has been largely thought of as dispensable for vascular development in vertebrates. Here, we generated a zebrafish *vegfd* mutant by genome editing. *vegfd* mutants display significant defects in facial lymphangiogenesis independent of *vegfc* function. Strikingly, we find that *vegfc* and *vegfd* cooperatively control lymphangiogenesis throughout the embryo, including during the formation of the trunk lymphatic vasculature. Interestingly, we find that *vegfd* and *vegfc* also redundantly drive artery hyperbranching phenotypes observed upon depletion of Flt1 or Dll4. Epistasis and biochemical binding assays suggest that, during primary angiogenesis, Vegfd influences these phenotypes through Kdr (Vegfr2) rather than Flt4 (Vegfr3). These data demonstrate that, rather than being dispensable during development, Vegfd plays context-specific indispensable and also compensatory roles during both blood vessel angiogenesis and lymphangiogenesis.

KEY WORDS: Vegfd, Vegfc, Flt4, Kdr, Lymphatic, Lymphangiogenesis

INTRODUCTION

Signaling through the VEGF/VEGFR pathway is essential for multiple steps during development of the vasculature. In zebrafish, primary angiogenesis occurs when arterial sprouts emerge from the dorsal aorta (DA) from ∼22 hpf to give rise to the intersegmental arteries (aISV) in a process dependent on Kdr, Kdrl and Vegfa (Bahary et al., 2007; Covassin et al., 2006; Lawson et al., 2002; Lawson and Weinstein, 2002; Nasevicius et al., 2000; Olsson et al., 2006). During primary angiogenesis, blood vessel sprouting is led by tip cells, which express high levels of Flt4 (Vegfr3 in mammals) and display active Erk signaling (Gore et al., 2011; Shin et al., 2016a). In zebrafish, whole-genome duplication has resulted in the presence of two Vegfr2 paralogs, Kdr and Kdrl (Bussmann et al., 2008; Covassin et al., 2006). Tip cells are highly responsive to Kdr, Kdrl and Flt4 signaling, and have low Notch-signaling activity. In the zebrafish, the loss of Dll4, a Notch ligand, leads to increased angiogenic sprouting (Leslie et al., 2007; Siekmann and Lawson, 2007). Dll4 negatively regulates arterial Flt4 signaling and suppresses the arterial response to Vegfc (Hogan et al., 2009b; Villefranc et al., 2013). Likewise, Flt1 (Vegfr1) also plays a negative regulatory role, its soluble form (sFlt1) suppresses arterial Vegfr signaling and angiogenesis, with morpholino (MO) knockdown of Flt1 leading to aISV hyperbranching (Krueger et al., 2011). Although Vegfa plays the dominant role in controlling arterial sprouting and Vegfc has been shown to influence this process, Vegfd has not previously been implicated in the regulation of primary sprouts (Hogan et al., 2009b; Jakobsson et al., 2010; Siekmann and Lawson, 2007).

The sprouting of both venous intersegmental vessels (vISV) and lymphatic endothelial cells (LECs) occurs by secondary angiogenesis from ∼32 hpf in zebrafish (Isogai et al., 2003). Sprouts emerging from the cardinal vein can become vISVs or LECs when they either anastomose with existing aISVs to form vISVs, or fail to anastomose and migrate dorsally to form parachordal LECs at the horizontal myoseptum (HM) (Isogai et al., 2003; Koltowska et al., 2013, 2015). Parachordal LECs in the HM proliferate and migrate dorsally and ventrally to form the major trunk lymphatics: the thoracic duct (TD), dorsal longitudinal lymphatic vessel (DLLV) and the intersegmental lymphatic vessels (ISLVs) (Cha et al., 2012; Hogan et al., 2009b; Küchler et al., 2006; Yaniv et al., 2006). Facial lymphangiogenesis proceeds from the common cardinal vein (CCV) as lymphatic sprouts migrate to form the lateral facial lymphatic (LFL), medial facial lymphatic (MFL) and the otolithic lymphatic vessel (OLV) by 5 dpf (Okuda et al., 2012). The formation of zebrafish lymphatic vessels is dependent on the Ccbe1/Vegfc/Flt4 signaling axis (Hogan et al., 2009a; Le Guen et al., 2014; Villefranc et al., 2013). Vegfd has been shown by MO knockdown to compensate for loss of Vegfc during facial lymphatic development but not elsewhere in the embryo (Astin et al., 2014). Growth factor-induced signaling downstream of Flt4 occurs through the activation of Erk, which is necessary and sufficient in the trunk to induce the normal sprouting of LECs and expression of the LEC marker Prox1 (Koltowska et al., 2015; Shin et al., 2016b). During facial lymphangiogenesis from the CCV, Erk signaling controls LEC sprouting but not Prox1 expression, suggesting spatially distinct mechanisms that remain to be fully understood (Shin et al., 2016b).

VEGFD is structurally related to VEGFC and can signal through both VEGFR3 and VEGFR2 in humans but only through Vegfr3 in mice (Achen et al., 1998; Baldwin et al., 2001a). Overexpression of VEGFD in tumor cells induces tumor angiogenesis, lymphangiogenesis and the dilation of collecting lymphatic vessels, ultimately promoting the metastatic spread of tumor cells (Karnezis et al., 2012; Stacker et al., 2002, 2001; Von Marschall

[1]Division of Genomics of Development and Disease, Institute for Molecular Bioscience, The University of Queensland, St Lucia, Brisbane, Queensland 4072, Australia. [2]Tumour Angiogenesis and Microenvironment Program, Peter MacCallum Cancer Centre, Melbourne, Victoria 3000, Australia. [3]Sir Peter MacCallum Department of Oncology, The University of Melbourne, Melbourne, Victoria 3010, Australia.

*Author for correspondence (b.hogan@imb.uq.edu.au)

B.M.H., 0000-0002-0651-7065

Received 14 November 2016; Accepted 19 December 2016

Development (2017) 144, 507-518 doi:10.1242/dev.146969

et al., 2005). Expression of VEGFD in solid human tumors is a strong indicator of metastasis and poor prognosis (Achen et al., 2005; Stacker et al., 2014). However, despite this potent capability of VEGFD, its function during embryonic development has remained unclear. *Vegfd* knockout mice on a mixed genetic background are viable with no obvious defects in blood or lymphatic endothelium (Baldwin et al., 2005). *Vegfc, Vegfd* double-knockout mice display a developmental phenotype that appears to be the same as that of *Vegfc* knockout mice (Haiko et al., 2008), hence it is considered that *Vegfd* is not involved during embryonic development. However, postnatal phenotypes have been observed in some tissues and include a reduction in the abundance of pulmonary lymphatics (Baldwin et al., 2005) and, in adult mice of a pure C57BL/6 background, smaller initial dermal lymphatics and compromised function (Paquet-Fifield et al., 2013).

We have recently found that *vegfd* is expressed throughout the embryonic trunk during zebrafish development (Duong et al., 2014), suggesting a potential function that remains to be fully explored. Here, we report the generation of a zebrafish *vegfd* mutant. *vegfd* is dispensable for development of trunk blood and lymphatic vessels. However, we find that *vegfd* is essential for normal facial lymphangiogenesis and combines with *vegfc* contextually during lymphangiogenesis throughout the trunk and face. Furthermore, Vegfc and Vegfd together influence aISV development in a number of knockdown or overexpression settings. In this context, Vegfd is likely to act through Kdr, which we find binds to Vegfd in zebrafish. These findings identify Vegfd as a developmental regulator of both lymphangiogenesis and angiogenesis.

RESULTS

Generation of a zebrafish *vegfd* mutant

To investigate the developmental role of Vegfd, we used TALEN mutagenesis to generate a zebrafish mutant harboring a 7 bp deletion at base 162 of the *vegfd*-coding sequence. The deletion site is in an exon common to both of the known protein-coding transcript variants that contain the Vegfd homology domain (VHD). The 7 bp deletion introduces a stop codon at amino acid 65, which is prior to the VHD of the Vegfd protein and is predicted to result in a null mutant (Fig. 1A,B). Analysis of the number of aISVs, vISVs and the extent of the TD in the trunks of *vegfd*^{uq9bh} mutant embryos revealed no differences between homozygous mutant, heterozygous or wild-type embryos (Fig. 1C,D, Fig. S1A,B). *vegfd*^{uq9bh} homozygous mutant embryos were raised to adulthood and produced viable offspring (Fig. 1E-H). Analysis of *vegfd* mRNA levels in embryos derived from in-crosses of *vegfd* homozygous mutant adults showed that these mutant embryos had less than 50% of the transcript levels of stage-matched wild-type embryos, indicative of nonsense-mediated decay (NMD) (Fig. S1C). Additionally, we did not observe any change in *vegfc* mRNA levels in *vegfd*^{uq9bh} homozygous mutants, indicating that compensation for the loss of *vegfd* is unlikely to occur (Fig. S1C).

Vegfd morpholino (MO) knockdown has previously been reported and revealed that Vegfd compensates for the loss of facial lymphatics in *vegfc*^{hu5055} mutants (Astin et al., 2014). We performed the reciprocal experiment, injecting a *vegfc* MO into embryos produced from a cross of homozygous with heterozygous *vegfd*^{uq9bh} mutants. Using an approach blinded for genotype, we scored injected embryos as displaying 'severe' (defined as a complete loss of the MFL and LFL) or 'partial' (indicating reduced length of the MFL and LFL) phenotypes and found *vegfd*^{uq9bh} mutants were enriched in the 'severe loss' category of embryos, confirming previous findings and suggesting that these mutants did not express functional Vegfd (Fig. S1D,E). Taking into account this phenocopy of the MO-induced defects, the nature of the mutation and detection of NMD, we suggest that the *vegfd*^{uq9bh} allele is a loss-of-function allele and likely to be null.

Vegfd regulates lymphangiogenesis of the facial lymphatic network

To more accurately characterize the role of Vegfd during development of the facial lymphatics, we generated *vegfd*^{uq9bh}, *vegfc*^{hu5055} double mutants in a *Tg(fli1a:negfp), Tg(-5.2lyve1b:dsRed)* transgenic background. This previously reported *vegfc*^{hu5055} mutant is hypomorphic and displays a strong but variable loss of lymphatics (Le Guen et al., 2014). The number of individual nuclei in each of the different facial lymphatic vessels was quantified in embryos from *vegfd*^{uq9bh}, *vegfc*^{hu5055} double heterozygous in-crosses (Fig. 1J-Q). In double mutant embryos, the facial lymphatics failed to develop (Fig. 1N). Strikingly, *vegfd*^{uq9bh} mutant embryos displayed fewer facial lymphatic nuclei in the LFL and MFL than in wild-type embryos, without any reduction in *vegfc* gene dose (Fig. 1L,O,P). There were also significantly fewer nuclei in *vegfc*^{hu5055}, *vegfd*^{uq9bh} double heterozygotes compared with wild-type embryos for both the LFL and MFL (Fig. 1K,O,P). Vegfd did not contribute to the formation of the otolithic lymphatic vessel (OLV), which was *vegfc* dependent (Fig. 1Q). Together, these data show that *vegfd* regulates development of the facial lymphatics, specifically the MFL and LFL, and that combined gene dose for *vegfc* and *vegfd* is essential for the formation of the complete facial lymphatic network.

Vegfd contributes to formation of the trunk lymphatic vessels

vegfd^{uq9bh} mutant embryos develop normal trunk lymphatics in a *vegfc* wild-type background (Fig. 1D, Fig. S1A). To determine whether *vegfd* works together with *vegfc* in this context, we examined the formation of parachordal LECs in the *vegfc*^{hu5055} hypomorphic mutant in a *vegfd*^{uq9bh} mutant background (Fig. 2A-F). In siblings that were homozygous wild type for the *vegfc*^{hu5055} allele, the loss of a single copy or both copies of *vegfd* did not produce any lymphatic phenotype, indicating that Vegfd is dispensable for normal trunk lymphangiogenesis in the presence of wild-type levels of Vegfc (Fig. 2A,D). However, in a *vegfc*^{hu5055} heterozygous background, *vegfd*^{uq9bh} homozygous and heterozygous mutants developed significantly fewer parachordal LECs than *vegfd*^{uq9bh} wild-type embryos, demonstrating a compensatory role for Vegfd with reduced gene dose for *vegfc* (Fig. 2E). Analysis of *vegfd*^{uq9bh} allelic loss in a *vegfc*^{hu5055} homozygous mutant background did not reveal further significant interactions (Fig. 2F).

We next scored the extent of the TD across nine somites at 5 dpf. In siblings that were homozygous wild type for the *vegfc*^{hu5055} allele, the loss of a single or both copies of *vegfd* again did not produce a lymphatic phenotype (Fig. 3A,B). In both *vegfc*^{hu5055} heterozygous and homozygous mutant backgrounds, *vegfd*^{uq9bh} homozygous loss led to significantly reduced TD extent (Fig. 3C-F,H,I). To more accurately quantify the loss of TD in *vegfd*^{uq9bh}, *vegfc*^{hu5055} double mutant backgrounds, we precisely scored the number of nuclei present in the TD across 9 somites using the *Tg(fli1a:negfp), Tg(-5.2lyve1b:dsRed)* transgenic strain (Fig. 3J-L). We found that many hypomorphic *vegfc*^{hu5055} homozygous mutant embryos partially formed a TD; however, this was significantly reduced in the absence of *vegfd* (Fig. 3J-L). In the majority of cases, double mutants failed to form a single LEC in the region of the embryonic TD. Together, these data show a compensatory role for *vegfd* with *vegfc* during trunk

Development (2017) 144, 507-518 doi:10.1242/dev.146969

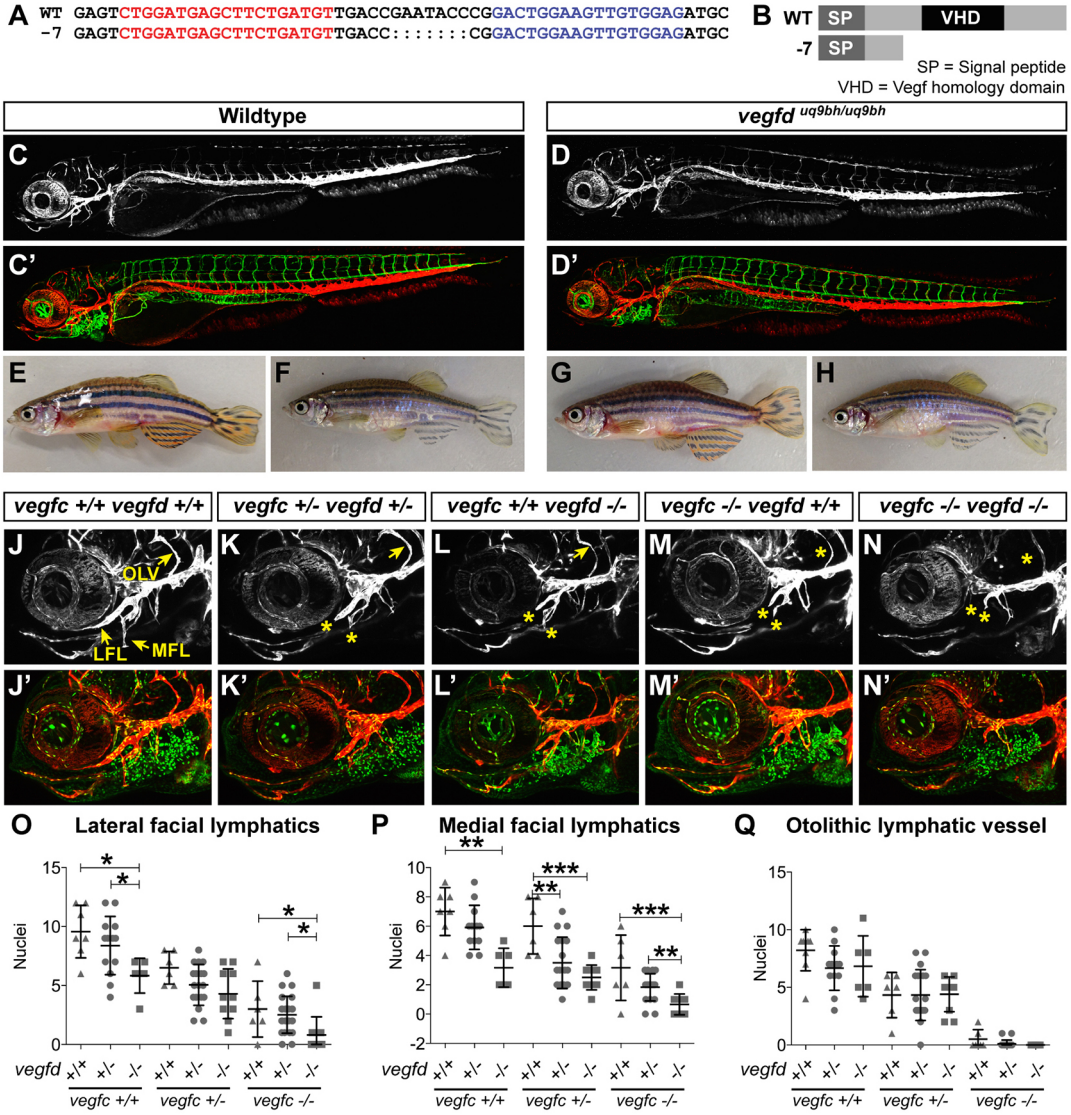

Fig. 1. *vegfd* regulates facial lymphangiogenesis. (A) Forward (red) and reverse (blue) Talens used to target the *vegfd* locus induced a 7 bp deletion designated as the *uq9bh* allele. (B) The *uq9bh* allele results in a premature stop codon at amino acid 65, prior to the VEGF homology domain. (C,D) Confocal images of *Tg(-5.2lyve1b:dsRed)*;*Tg(flt1:yfp)* wild-type (C, *lyve1b:dsRed* only; C′) and *vegfd*^{uq9bh} mutant embryos (D, *lyve1b:dsRed* only; D′) at 5 dpf. (E-H) *vegfd*^{uq9bh} adult mutants are viable and have no obvious defects (G,H) when compared with siblings (E,F). (J-N′) Confocal images showing the facial region of 5 dpf *Tg(fli1a:negfp);Tg(-5.2lyve1b:dsRed)* transgenic embryos produced by in-crossing *vegfd*^{uq9bh}, *vegfc*^{hu5055} double heterozygotes. Arrows indicate the presence of normal medial facial lymphatics (MFL), lateral facial lymphatics (LFL) and otolithic lymphatic vessel (OLV). Asterisks indicate the reduction of LEC number in these vessels. (O-Q) *vegfd*^{uq9bh} mutant embryos have a reduced number of facial lymphatic endothelial cells (LECs) when quantified in 5 dpf *Tg(fli1a:negfp):Tg(-5.2lyve1b:dsRed)* embryos. (O) Significant differences in LFL LEC numbers were observed when *vegfd*^{uq9bh} mutants (n=5) were compared with *vegfd*^{uq9bh} heterozygous (n=12) or wild-type (n=7) embryos in a *vegfc*^{hu5055} wild-type background; and when *vegfd*^{uq9bh} mutants (n=7) were compared with *vegfd*^{uq9bh} heterozygous (n=18) or wild-type (n=6) embryos in *vegfc*^{hu5055} mutants. (P) Significant differences in MFL LEC numbers were observed when comparing *vegfd*^{uq9bh} mutants (n=6) with *vegfd*^{uq9bh} wild-type (n=7) embryos in a *vegfc*^{hu5055} wild-type background; when comparing *vegfd*^{uq9bh} mutant (n=10) or heterozygous embryos (n=18) with *vegfd*^{uq9bh} wild type (n=6) and embryos in a *vegfc*^{hu5055} heterozygous background; and when *vegfd*^{uq9bh} mutants (n=9) were compared with *vegfd*^{uq9bh} heterozygous (n=18) and wild-type (n=6) embryos in a *vegfc*^{hu5055} mutant background. (Q) There was no interaction between *vegfc* and *vegfd* in the formation of the otolithic lymphatic vessel. Data represent mean±s.e.m.; ***P<0.001, ** P<0.01, *P<0.05 from one-way ANOVA from three independent clutches of embryos.

lymphangiogenesis, although *vegfc* alone is sufficient to generate a trunk lymphatic vasculature during development.

Given the known and suggested biochemical interactions between Flt4, Ccbe1 and Vegfd in zebrafish and in mammals, we next examined whether there were genetic interactions between mutants for these components during the formation of the TD. We analyzed TD formation in embryos from *vegfd*^{uq9bh}, *flt4*^{hu4602} and *vegfd*^{uq9bh}, *ccbe1*^{hu3613} double heterozygous in-crosses at 7 dpf. *ccbe1*^{hu3613} homozygous mutant embryos had a complete loss of the TD irrespective of *vegfd*^{uq9bh} genotypic status and we were unable to detect any genetic interaction in these crosses (data not shown). Analysis of TD formation in embryos from *vegfd*^{uq9bh}, *flt4*^{hu4602} double heterozygous in-crosses revealed that, in a *flt4*^{hu4602} heterozygous background, *vegfd*^{uq9bh} mutants had significantly reduced TD formation compared with *vegfd*^{uq9bh} heterozygous or wild-type embryos (Fig. 3M-O). Hence, the *flt4*^{hu4602} mutation dominantly interacts with the *vegfd*^{uq9bh} mutation, which does not normally result in a TD phenotype.

Development (2017) 144, 507-518 doi:10.1242/dev.146969

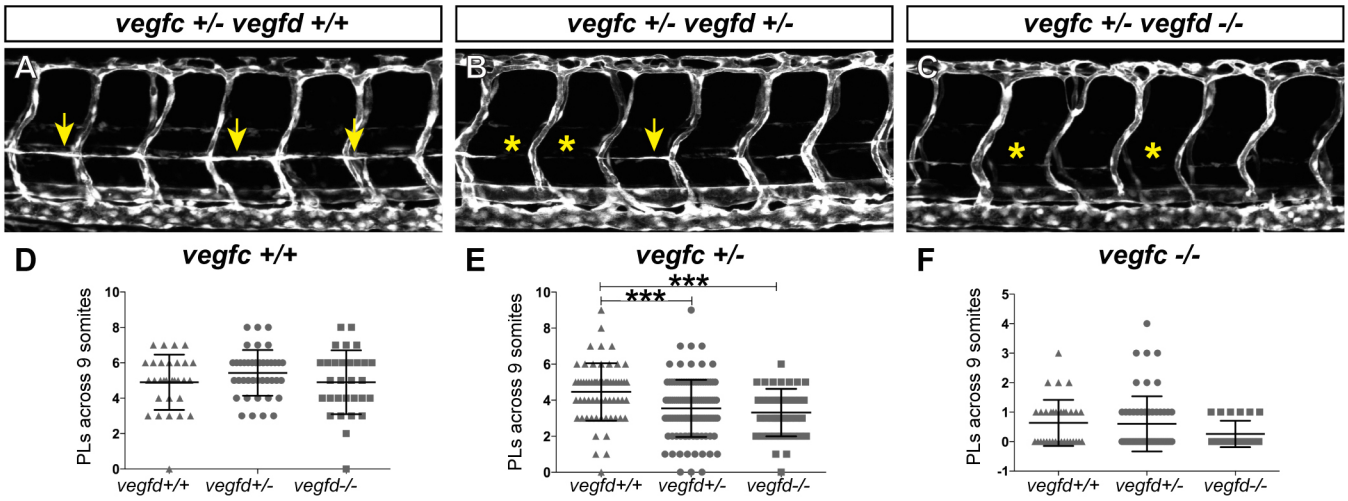

Fig. 2. Vegfd contributes to the development of parachordal lymphatic endothelial cells. (A-C) Confocal images at 54 hpf showing presence (arrows) or absence (asterisks) of PL formation in representative *Tg(fli1a:egfp) vegfc*^{hu5055}, *vegfd*^{uq9bh} mutant embryos. (D-F) Quantification of PL formation in *vegfd*^{uq9bh} mutant embryos in *vegfc*^{hu5055} wild-type (D), heterozygous (E) and mutant (F) backgrounds. There were significantly fewer PLs formed in *vegfd*^{uq9bh} homozygous mutant (*n*=42) and heterozygous (*n*=112) embryos when compared with *vegfd*^{uq9bh} wild-type (*n*=63) embryos in a *vegfc*^{hu5055} heterozygous background (E). Error bars represent mean±s.e.m.; ***P<0.001 from one-way ANOVA from three independent clutches of embryos.

Arterial defects induced by Vegfd overexpression are Kdr (Vegfr2) dependent

VEGFC and VEGFD are capable of signaling through VEGFR3 (Flt4 in zebrafish) or VEGFR2 (Kdr and Kdrl in zebrafish) in different settings (Achen et al., 1998; Covassin et al., 2006; Hogan et al., 2009b; Joukov et al., 1996; Karnezis et al., 2012; Le Guen et al., 2014; Villefranc et al., 2013). Overexpression of *vegfd* or *vegfc* by mRNA injection in zebrafish causes bilateral turning of the aISVs at 28-32 hpf (Astin et al., 2014; Hogan et al., 2009b). We co-injected *vegfd* mRNA with a *flt4* MO and found no decrease in the number of turned aISVs when compared with *vegfd* mRNA injection alone (Fig. 4B,F,I), whereas co-injection of *flt4* morpholino with *vegfc* mRNA led to a rescue of the *vegfc* mRNA-driven phenotype, as previously reported (Hogan et al., 2009b) (Fig. S2A,B). To determine which receptor Vegfd is likely signaling through, we co-injected *vegfd* mRNA with morpholinos targeting other Vegf receptors. Importantly, we ensured that each of these MOs was efficacious by using previously published MOs and reproducing previously validated phenotypes. Specifically for the MOs used in this study, ISV hyperbranching is robustly induced using the *flt1* MO (Krueger et al., 2011) and the *dll4* MO (Hogan et al., 2009b; Siekmann and Lawson, 2007); the *kdr* and *kdrl* MO combined robustly block ISV development (but neither alone achieves this) (Covassin et al., 2006; Wiley et al., 2011); and the *flt4* MO blocks the formation of lymphatic vessels in a highly reproducible manner (Hogan et al., 2009b). Co-injection of the *flt1* MO with *vegfd* mRNA led to an increase in the number of turned aISVs at 28-32 hpf compared with embryos injected with *vegfd* mRNA alone (Fig. 4B,G,H,J). Flt1 is known to suppress Vegfa signaling through Vegfr2 (Kdr or Kdrl in zebrafish) (Krueger et al., 2011; Wiley et al., 2011), but enhancement of the hyperbranching phenotype by *vegfd* overexpression is unexpected. Co-injection of *vegfd* mRNA with *kdr* MO rescued the bilateral turning of the aISV phenotype at 28-32 hpf (Fig. 4B,C,I), whereas injection with *kdrl* MO failed to rescue (data not shown). We also co-injected *vegfc* mRNA with *kdr* MO and found no rescue of the *vegfc*-driven phenotype (Fig. S2B). It has previously been reported that overexpression of Vegfd leads to an upregulation of *Vegfr2* in rabbit blood vessels (Rissanen et al., 2003), which could contribute to the ectopic turning of aISVs in this setting. To examine this, we performed qPCR on 28 hpf *vegfd* mRNA-injected embryos and controls; we found no significant changes in the expression of *kdr*, *kdrl*, *flt4*, *vegfaa*, *vegfab*, *dll4*, *flt1* or *fli1a* (Fig. 4K). Together, these data suggest that in the context of zebrafish aISV development, Vegfc and Vegfd are capable of acting through Flt4 and Kdr, respectively.

Zebrafish Vegfd is proteolytically processed and binds Kdr

The genetic evidence presented above suggests that zebrafish Vegfd influences primary angiogenesis via interaction with Kdr. To further confirm this, we tested the capacity of zebrafish Vegfd to bind Kdr. Comparison of zebrafish and human VEGFD revealed that the zebrafish protein has a similar primary domain structure with N- and C-terminal propeptides flanking a central VEGF homology domain (VHD) (Fig. 5A). Previous studies with human (Stacker et al., 1999) and mouse (Baldwin et al., 2001b) VEGFD demonstrated that the N- and C-terminal propeptides can be proteolytically cleaved to generate a mature form consisting of dimers of the VHD. The mature form of human VEGFD has much higher affinity for human VEGFR2 compared with the full-length form (Stacker et al., 1999); furthermore, the proteolytic processing of VEGFD is important for its activity in disease settings (Harris et al., 2011). We therefore expressed a form of full-length zebrafish Vegfd tagged at the N-terminus with the FLAG octapeptide, designated zVegfd-FULL-N-FLAG, in transiently transfected human HEK293T cells to assess whether it can be proteolytically processed. Western blot analysis of conditioned media (CM) revealed the presence of bands at ∼47, 36 and 15 kDa (Fig. 5B, left panel), consistent with the expected sizes of full-length Vegfd, of a partially processed form containing the N-terminal propeptide and the VHD, and of a form consisting of only the N-terminal propeptide, respectively. These findings confirm that zebrafish Vegfd can be proteolytically processed, at least when expressed in mammalian cells.

Given that zebrafish Vegfd can be processed, and that the mature form of human VEGFD exhibits higher affinity for VEGFR2 than other forms of the growth factor, we used a mature form of zebrafish

Development (2017) 144, 507-518 doi:10.1242/dev.146969

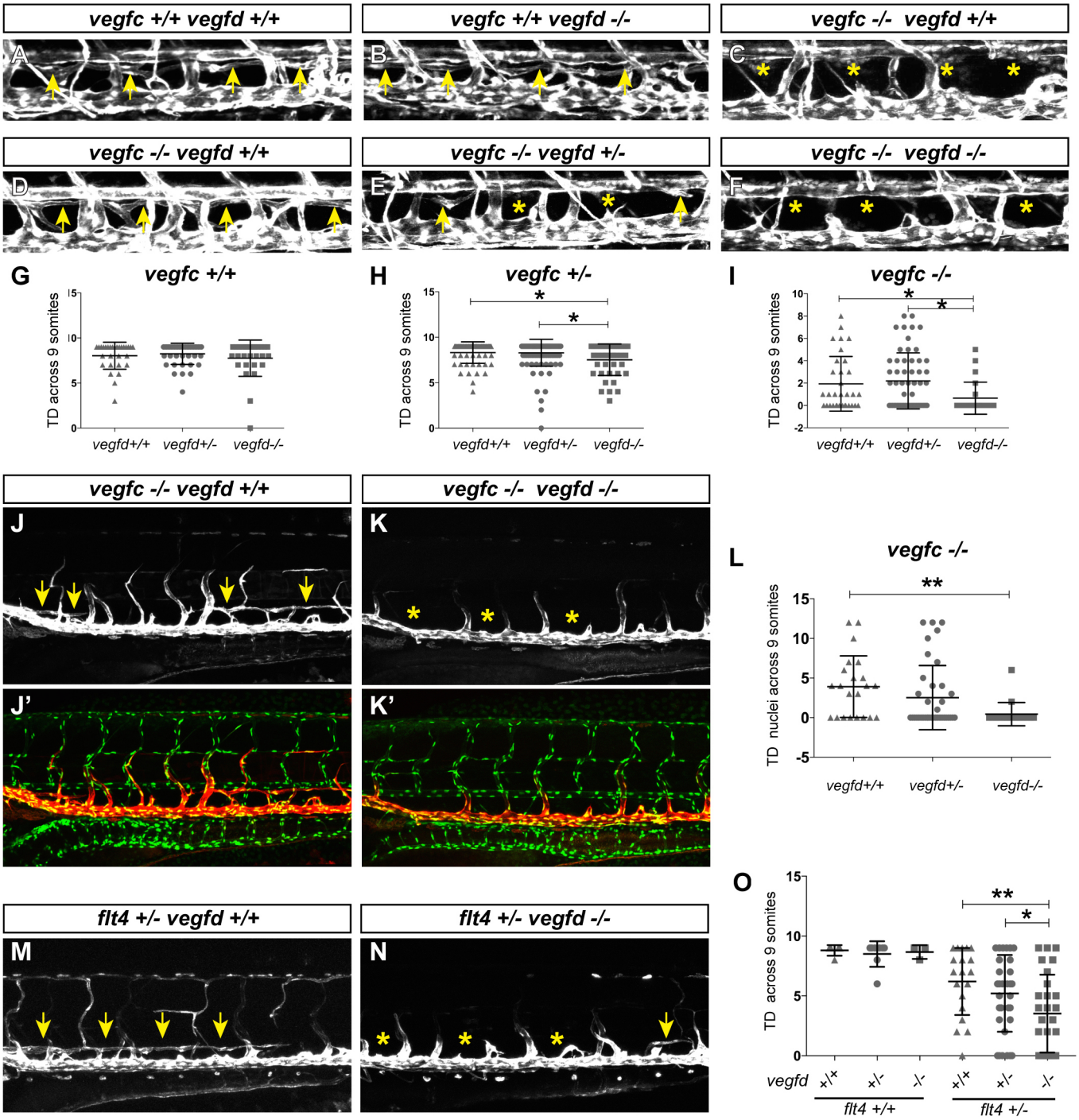

Fig. 3. Vegfd contributes to thoracic duct development in the zebrafish trunk. (A-F) Confocal images of *Tg(fli1a:egfp)* at 5 dpf showing formation of the TD (arrows) is normal in *vegfd*^{uq9b} mutants (A,B). The phenotype for the formation of the TD is variable in *vegfc*^{hu5055} mutants, ranging from a complete loss (C) to very mild loss (D). The formation of the TD is reduced (asterisk) in *vegfc*^{hu5055} mutants that were heterozygous (E) or mutant (F) for *vegfd*^{uq9bh}. (G-I) Quantification of TD extent across nine somites in *vegfd*^{uq9bh} mutant embryos in *vegfc*^{hu5055} wild-type (G), heterozygous (H) and mutant (I) backgrounds. There was significantly less TD formed in *vegfd*^{uq9bh} mutant embryos (n=42) when compared with *vegfd*^{uq9bh} heterozygous (n=112) and wild-type (n=63) embryos in a *vegfc*^{hu5055} heterozygous background (H); and in *vegfd*^{uq9bh} mutant embryos (n=25) when compared with *vegfd*^{uq9bh} heterozygous (n=56) and wild-type (n=33) embryos in a *vegfc*^{hu5055} homozygous mutant background (I). Data represent mean±s.e.m.; *P<0.05 from Kruskal–Wallis test from three independent clutches of embryos. (J-K′) Confocal images of TD formation in 5 dpf *Tg(fli1a:negfp),Tg(-5.2lyve1b:dsRed)* embryos showing that fragments of TD form in *vegfc*^{hu5055} mutant/*vegfd*^{uq9bh} wild-type embryos (J,J′), but are absent in *vegfc*^{hu5055}/*vegfd*^{uq9bh} double-mutant embryos (K,K′). (L) Quantification of experiment in J-K′. The number of nuclei present in the TD of *vegfd*^{uq9bh} mutant (n=14) embryos was significantly lower when compared with *vegfd*^{uq9bh} heterozygous (n=21) and *vegfd*^{uq9bh} wild-type (n=13) embryos in a *vegfc*^{hu5055} mutant background. Data represent mean±s.e.m.; **P<0.01, from one-way ANOVA from three independent clutches of embryos. (M,N) Confocal images of TD formation in 7 dpf *Tg(-5.2lyve1b:dsRed)* embryos (yellow arrows) in a *flt4*^{hu4602} heterozygous background. *vegfd*^{uq9bh} mutants (N) have reduced TD formation compared with *vegfd*^{uq9bh} wild-type embryos (M). (O) Quantification of experiment in M,N. There was significantly less TD formed in *vegfd*^{uq9bh} mutant embryos (n=33) when compared with *vegfd*^{uq9bh} heterozygous (n=19) and wild-type embryos (n=27) in a *flt4*^{hu4602} heterozygous background. **P<0.01, *P<0.05 from Kruskal–Wallis test from three independent clutches of embryos.

Development (2017) 144, 507-518 doi:10.1242/dev.146969

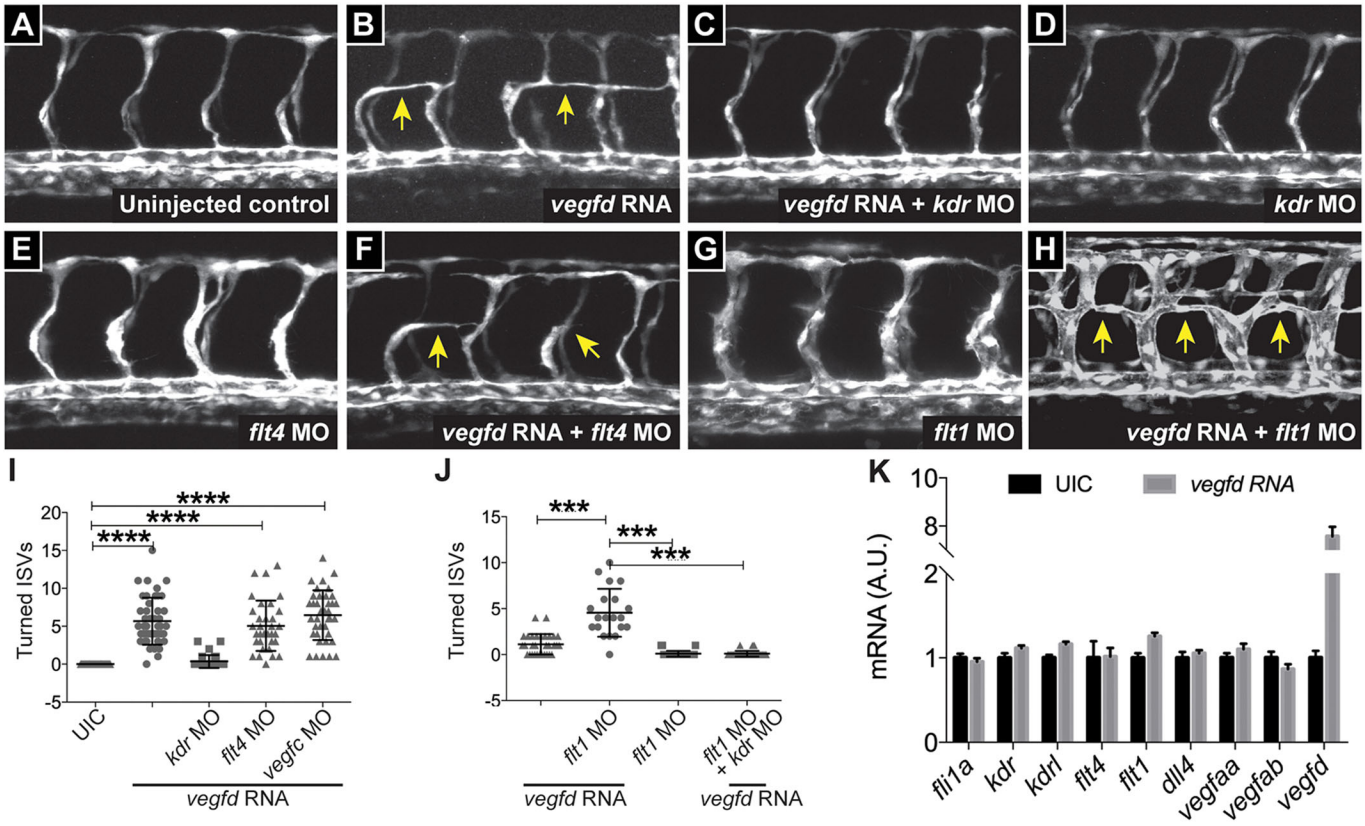

Fig. 4. Vegfd mRNA injection induces artery defects in a Kdr-dependent manner. (A-F) Injection of *vegfd* RNA into *Tg(fli1a:egfp)* embryos causes bilateral turning of aISVs (arrows) at 28-32 hpf (*n*=31, A,B), which is rescued by co-injection of a morpholino against *kdr* (C,D), but not *flt4* morpholino injection (E,F). (G,H) Co-injection of *flt1* morpholino and *vegfd* RNA increases the bilateral turning of aISVs (*n*=20) when compared with *vegfd* RNA (*n*=31) or *flt1* morpholino alone (*n*=29) (compare A,B,G and H). (I,J) Quantification of experiments presented in A-E (I) and G,H (J). Data represent mean±s.e.m.; ****P<0.0001, ***P<0.001 from one-way ANOVA. Data were obtained from three independent injections. (K) qPCR analysis of *vegf* receptor and ligand expression in uninjected and *vegfd* mRNA-injected embryos shows no significant difference in mRNA levels for any of the genes examined.

Vegfd, consisting of the VHD, for receptor-binding studies. A version of mature zebrafish Vegfd tagged at the N-terminus with FLAG, designated zVegfdΔNΔC-FLAG, was expressed in transiently transfected HEK293T cells – the size of the subunits of this glycoprotein was in the 21-28 kDa range (Fig. 5B, right panel), as expected based on the sizes of mature human and mouse Vegfd (Achen et al., 1998; Baldwin et al., 2001b). CM containing zVegfdΔNΔC-FLAG were incubated with Ig-fusion proteins, consisting of the extracellular domains of zebrafish Kdr or Kdrl and the Fc region of mouse IgG, that were bound to protein A-sepharose (see Materials and Methods). Western blotting of material precipitated by the Ig-fusion proteins/protein A-sepharose revealed that the Kdr extracellular domain could bind zVegfdΔNΔC-FLAG, whereas the extracellular domain of Kdrl could not (Fig. 5C, left panel). Hence, in line with our epistasis data above, mature Vegfd can bind Kdr, but not Kdrl in zebrafish.

Vegfd is dispensable for early primary angiogenic sprouting

As our data suggest that Vegfd is capable of signaling through Kdr, it is possible that *vegfd*^{uq9bh} mutants, upon loss of Kdrl, would show arterial defects similar to the loss of Kdr and Kdrl together (Wiley et al., 2011). To test this, we injected the *kdrl* MO into embryos derived from a homozygous *vegfd*^{uq9bh} mutant crossed to a heterozygous *vegfd*^{uq9bh} carrier. We independently quantified the number of aISVs that extended fully from the DA to the DLAV and the number of aISVs that had failed to sprout from the DA at 28 hpf (Fig. S3A,B). We found no significant difference in the number of aISVs between mutants or siblings upon Kdrl knockdown, suggesting that Vegfa plays a dominant role in aISV sprouting (Fig. S3A,B).

Given that *vegfc* mutants have been shown to interact genetically with *kdrl* during primary angiogenesis (Villefranc et al., 2013), we also examined the number of cells in the aISVs in *vegfc*^{hu5055}, *vegfd*^{uq9bh} double mutants at 28 hpf using the *Tg(fli1a:negfp)* transgenic background; however, we did not find any significant difference (Fig. S3C). This implies that Vegfa plays a more potent role than Vegfd. Although Vegfd is dispensable for early primary angiogenic sprouting, the ability to signal through Kdr when overexpressed shows that Vegfd is capable of inducing angiogenesis, which may be important in pathological states or in some mutant or knockdown settings.

Dll4 suppresses Vegfd signaling in developing intersegmental arteries

In zebrafish, loss of the Notch ligand Dll4 leads to increased tip cells and angiogenic sprouting because Dll4 negatively regulates Vegfc-driven arterial Flt4 signaling (Hogan et al., 2009b; Siekmann and Lawson, 2007; Villefranc et al., 2013). However, in *vegfc* mutants injected with *dll4* MO some arterial hyperbranching was still observed, despite the *vegfc*^{um18} allele used being shown to be a null allele (Villefranc et al., 2013). We injected *dll4* MO into embryos from a *vegfc*^{hu5055}, *vegfd*^{uq9bh} double heterozygous incross and quantified hyperbranching of aISVs followed by retrospective genotyping of the embryos (Fig. 6A-E). Although there was no reduction in

Development (2017) 144, 507-518 doi:10.1242/dev.146969

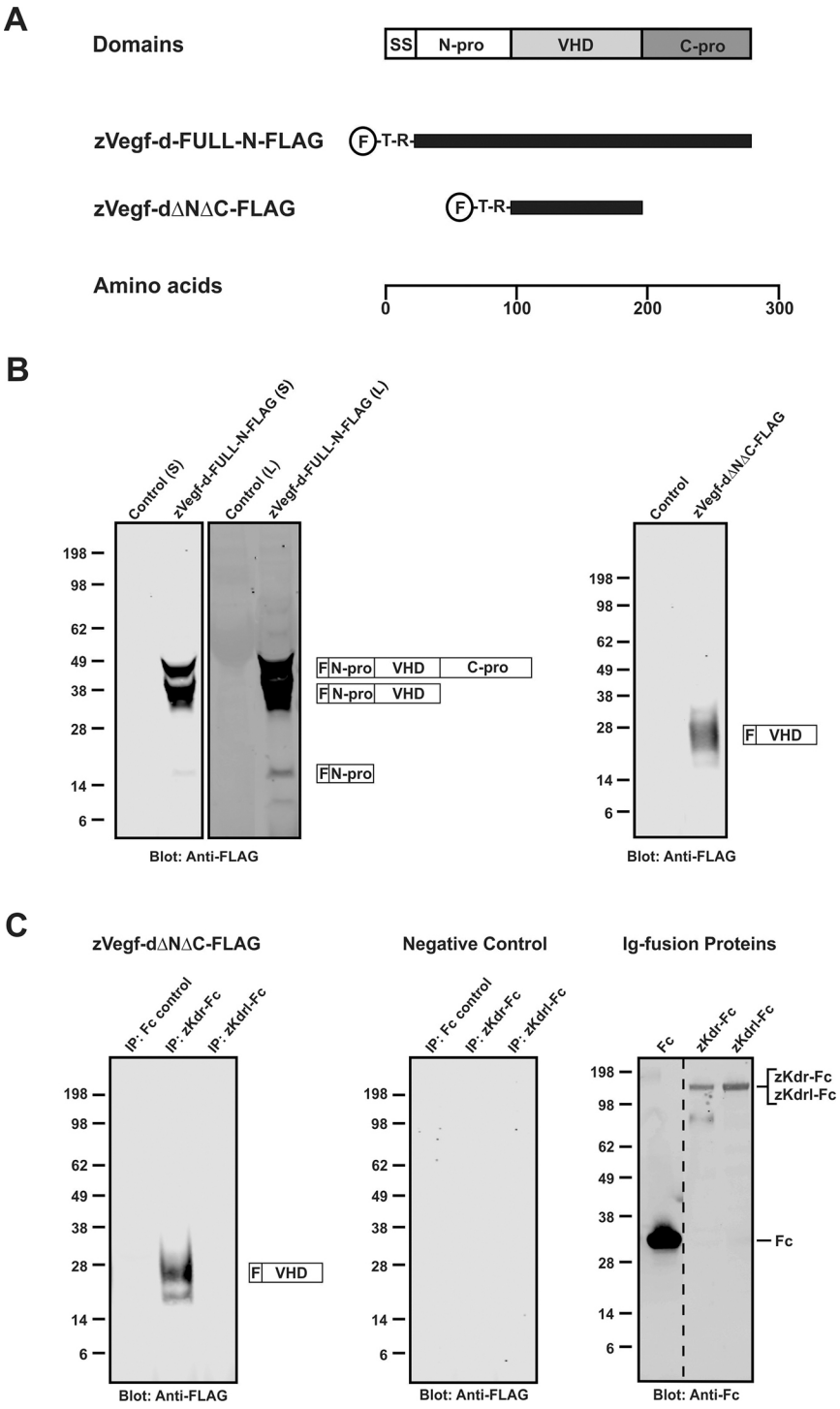

Fig. 5. Zebrafish Vegfd is proteolytically processed and binds Kdr. (A) Schematic map of the domain structure of zebrafish Vegfd and of Vegfd derivatives used in this study. In the domain map (top), SS denotes signal sequence for protein secretion; N-pro and C-pro denote N- and C-terminal propeptides, respectively; VHD denotes the VEGF homology domain. Primary translation products of zebrafish Vegfd derivatives zVegf-d-FULL-N-FLAG and zVegf-dΔNΔC-FLAG are depicted below but signal sequences are not shown. An encircled F indicates the FLAG octapeptide tag; other amino acids not present in zebrafish Vegfd are shown using single-letter code. (B) Analysis of zebrafish Vegfd expressed in human HEK293T cells. zVegf-d-FULL-N-FLAG and zVegf-dΔNΔC-FLAG were transiently expressed in HEK293T cells, and the resulting conditioned media (CM) analyzed by western blotting to detect the FLAG tag (zVegf-d-FULL-N-FLAG in the left panel; zVegf-dΔNΔC-FLAG in the right panel). Control indicates CM of cells transfected with expression vector lacking Vegfd. Two different exposures for detection of zVegf-d-FULL-N-FLAG are shown so that the FLAG tag and N-pro bands can be clearly visualized. (C) Analysis of the binding of mature zebrafish Vegfd to zebrafish Kdr and Kdrl. zVegf-dΔNΔC-FLAG was precipitated from the CM of transfected HEK293T cells using soluble Ig-fusion proteins consisting of the extracellular domains of zebrafish Kdr or Kdrl and the Fc region of mouse IgG, or of the Fc region only (zKdr-Fc, zKdrl-Fc and Fc, respectively), and detected by western blotting for the FLAG tag under reducing conditions (left panel). Control precipitations were performed from CM of cells transfected with expression vector lacking DNA for Vegfd (negative control, center panel). A western blot with anti-mouse IgG was performed to detect the Fc regions of Ig-fusion proteins used in precipitation reactions (right panel). The positions of Fc, zKdr-Fc and zKdrl-Fc are indicated (the expected sizes are ~34, ~150 and ~150 kDa, respectively), and a dashed line indicates where irrelevant tracks have been excised from the image. The blot shows that similar levels of zKdr-Fc and zKdrl-Fc were included in precipitations. The identity of the band at ~80 kDa in the Kdr-Fc track is unknown but it may represent a proteolytically processed form of Kdr-Fc. In B and C, schematic representations of detected forms of zebrafish Vegfd, as inferred from previous studies on human and mouse Vegfd (Baldwin et al., 2001b; Stacker et al., 1999), are shown on the right (F indicates FLAG tag).

hyperbranching in *vegfd*^{uq9bh} mutants alone, there was a significant reduction of hyperbranching in *vegfd*^{uq9bh}, *vegfc*^{hu5055} double mutants compared with single *vegfc*^{hu5055} mutants (Fig. 6C-E). This suggests that Vegfc is sufficient to drive the phenotype, but Vegfd acts in a compensatory manner. We conclude that Dll4 suppresses both Vegfc and Vegfd signaling in developing intersegmental arteries.

Flt1 suppresses Vegfd and Vegfc signaling and interacts with Dll4 in developing intersegmental arteries

Vegfr1 (Flt1 in zebrafish) plays a negative regulatory role during angiogenesis, with its soluble form (sFlt1) suppressing arterial Vegfr signaling and the knockdown of Flt1 leading to arterial hyperbranching (Hiratsuka et al., 1998; Krueger et al., 2011). Given the known interaction between Dll4/Notch signaling and Flt1 (Jakobsson et al., 2010), and our observation that Flt1 knockdown enhances the *vegfd* mRNA injection phenotype (Fig. 4H), we injected *flt1* MO into embryos from a *vegfc*^{hu5055}, *vegfd*^{uq9bh} double heterozygous in-cross. In a *vegfc*^{hu5055} heterozygous background, we found significantly fewer hyperbranched aISVs in *vegfd*^{uq9bh} heterozygous and homozygous mutant embryos compared with wild-type sibling embryos at 72 hpf (Fig. 6F-J). In a *vegfc*^{hu5055} mutant background, there were also fewer hyperbranched aISVs in

Development (2017) 144, 507-518 doi:10.1242/dev.146969

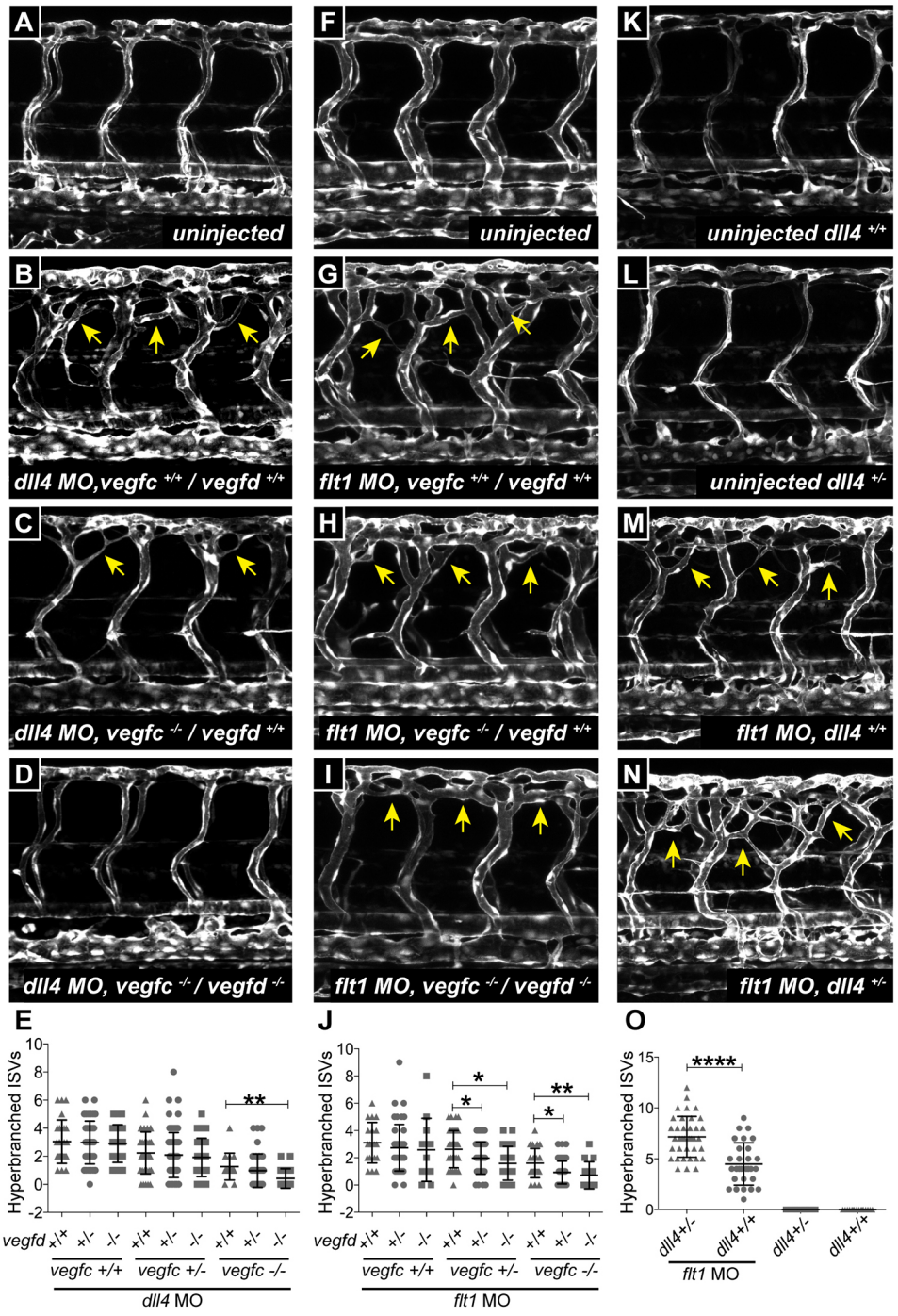

Fig. 6. Dll4 and Flt1 suppress Vegfc and Vegfd signaling in developing intersegmental arteries. (A-D) Confocal images of aISVs in 3 dpf *Tg(fli1a:egfp)* uninjected wild-type control (A), *dll4* morpholino (MO)-injected control (B), *dll4* MO-injected *vegfc*^{hu5055} mutant (C) and *dll4* MO-injected *vegfc*^{hu5055}, *vegfd*^{uq9bh} double mutant (D) embryos. Arrows indicate hyperbranching. (E) Quantification of hyperbranching in the experiment shown in A-D. *dll4* MO-injected *vegfc*^{hu5055}, *vegfd*^{uq9bh} double-mutant embryos (n=20) had significantly fewer hyperbranched aISVs than *dll4* MO-injected *vegfc*^{hu5055} mutants (n=15). (F-I) Confocal images of aISVs in 3 dpf *Tg(fli1a:egfp)* uninjected wild-type control (F), *flt1* MO-injected control (G), *flt1* MO-injected *vegfc*^{hu5055} mutant (H) and *flt1* MO-injected *vegfc*^{hu5055}, *vegfd*^{uq9bh} double-mutant embryos (I). Arrows indicate hyperbranching. (J) Quantification of hyperbranching in the experiment shown in F-I. *flt1* MO-injected *vegfc*^{hu5055}, *vegfd*^{uq9bh} double-mutant embryos (n=34) had significantly fewer hyperbranched aISVs than *vegfd*^{uq9bh} heterozygous (n=75) and wild-type (n=43) embryos in a *vegfc*^{hu5055} heterozygous background. *vegfd*^{uq9bh} mutant embryos (n=14) also had significantly fewer hyperbranched aISVs than *vegfd*^{uq9bh} heterozygous (n=52) and wild-type (n=23) embryos in a *vegfc*^{hu5055} mutant background. (K-N) Confocal images of aISVs in uninjected *Tg(fli1a:egfp)* wild-type embryos (n=21) (K), uninjected *dll4*^{uq10bh} heterozygous embryos (n=22) (L), *flt1* MO-injected wild-type embryos (n=37) (M) and *flt1* MO-injected *dll4*^{uq10bh} heterozygous embryos (n=29) (N) at 3 dpf. Arrows indicate hyperbranching. (O) Quantification of hyperbranching in the experiment shown in K-N. There was no hyperbranching of aISVs in *dll4*^{uq10b} heterozygous embryos compared with their wild-type siblings at 3 dpf (the phenotype initiates later in heterozygotes – see Fig. S3C). Hyperbranching was induced by 3 dpf following injection of *flt1* MO in wild-type embryos and the effect was significantly enhanced in *dll4*^{uq10b} heterozygous embryos. For all of the above analysis, data are mean±s.e.m.; ****P<0.0001, **P<0.01, *P<0.05 from one-way ANOVA. Data were obtained from three independent MO injections.

vegfd^{uq9bh} heterozygous and homozygous mutant embryos versus wild-type siblings (Fig. 6J). We also found less hyperbranching of aISVs when *vegfc*^{hu5055} heterozygous and mutant embryos were compared with wild-type siblings (Fig. S4A). These data indicates that Flt1 inhibits Vegfc and Vegfd signaling during primary angiogenesis, either directly or through its modulation of Vegfa signaling.

To further examine this scenario, we generated a *dll4* mutant harboring a 2 bp deletion at base 90 of the *dll4*-coding sequence. This deletion introduces a frame shift and a premature stop codon at amino acid 47 (Fig. S4B). We found that at 5 dpf *dll4*^{uq10bh} heterozygous embryos displayed mild hyperbranching of the intersegmental arteries, confirming *dll4* MO and hypomorphic mutant phenotypes (Fig. S4C) (Leslie et al., 2007; Siekmann and Lawson, 2007). *dll4* carriers had a poor survival rate of 6.25% in the F2 population. Given that the aISV hyperbranching in *flt1* morphant embryos was reduced in the *vegfc*^{hu5055}, *vegfd*^{uq9bh} double mutants, we injected the *flt1* MO into embryos from a *dll4*$^{uq10bh+/-}$ outcross and quantified the extent of artery hyperbranching at 72 hpf. This is a time point where the *flt1* MO injection induces hyperbranching of aISVs, but *dll4*^{uq10bh} heterozygous mutants do not show hyperbranching (Fig. 6G,L). We found that *dll4*^{uq10bh} heterozygosity significantly enhanced the hyperbranching of aISVs induced by *flt1* MO knockdown (Fig. 6N,O).

Finally, following our observations that the bilateral turning of arteries by *vegfc* and *vegfd* overexpression is Flt4 or Kdr dependent, respectively, we co-injected *kdr* and *flt1* MOs, and also *flt4* and *flt1*

Development (2017) 144, 507-518 doi:10.1242/dev.146969

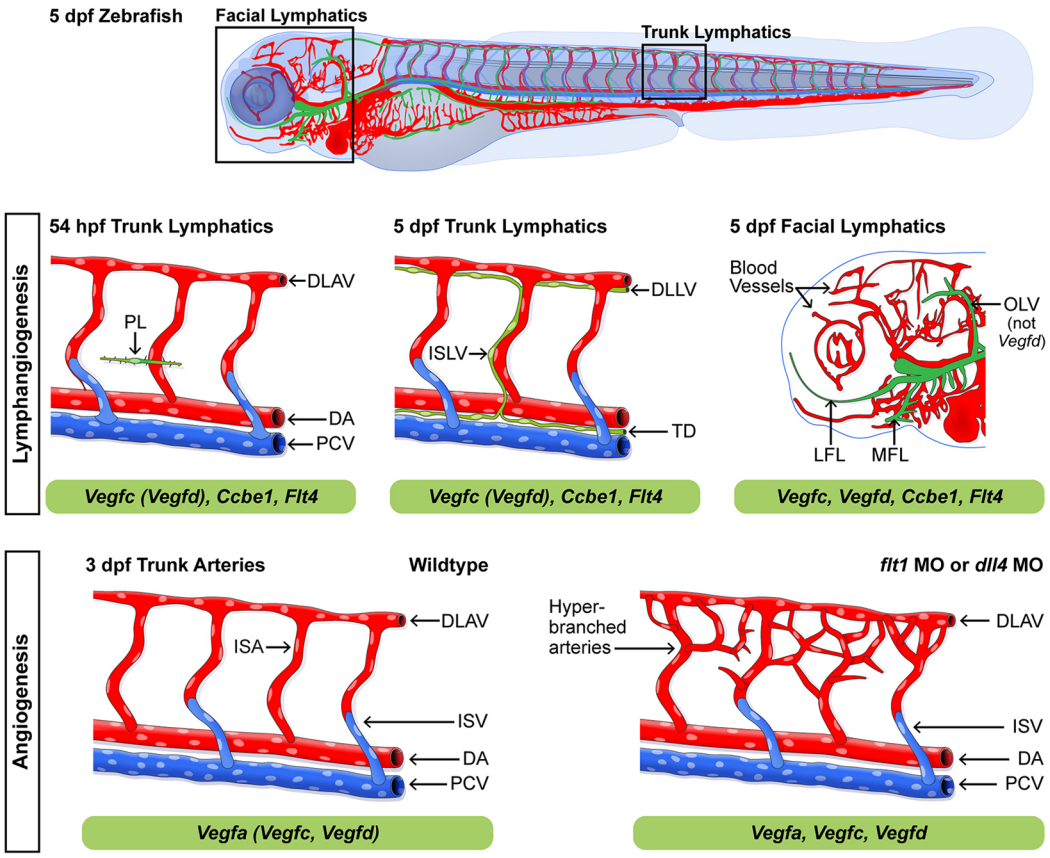

Fig. 7. Working model showing major contributors to Vegf signaling-mediated angiogenesis and lymphangiogenesis in zebrafish. Factors shown in brackets play redundant or compensatory roles; factors not in brackets are indispensable. Vegfd can compensate for reduced but not absent Vegfc during trunk lymphangiogenesis. However, during facial lymphangiogenesis Vegfd has an indispensable role in formation of the MFL and LFL but not the OLV. The combined gene dose of *vegfc* and *vegfd* is essential for the development of the complete, normal facial lymphatic network. During primary angiogenesis, the *Flt1* knockdown phenotype (shown in the schematic) and *Dll4* knockdown phenotype (not shown) are driven by Vegfc and Vegfd signaling, although Vegfc and Vegfd are dispensable for normal artery development. DLAV, dorsal longitudinal anastomosing vessel; PL, parachordal LEC; DA, dorsal aorta; PCV, posterior cardinal vein; DLLV, dorsal longitudinal lymphatic vessel; ISLV, intersegmental lymphatic vessel; TD, thoracic duct; aISV, arterial intersegmental vessel; vISV, venous intersegmental vessel.

MOs and found a significant reduction in hyperbranching in each of these separate co-injection scenarios compared with *flt1* MO only (Fig. S4D). Consistent with *vegfc* having the greatest impact on hyperbranching in mutant analyses (Fig. 6J), Flt4 knockdown produced the most significant reduction in this experiment (Fig. S4D). These data, combined with the findings above further demonstrate that *flt1* genetically interacts with *vegfc* and *vegfd*.

DISCUSSION

A role for Vegfd in developmental angiogenesis and lymphangiogenesis

Here, we describe a zebrafish *vegfd* mutant produced by Talen-induced mutagenesis. The *vegfd*^{uq9bh} mutant is viable and displays no obvious defects in primary or secondary angiogenesis in the trunk. This mutant is most likely a null, based on the nature of the mutation, an interaction with *vegfc* compared with published loss-of-function data (Astin et al., 2014) and NMD of the *vegfd* transcript. VEGFD has been widely considered to be dispensable for developmental lymphangiogenesis based on studies in knockout mice (Baldwin et al., 2005; Haiko et al., 2008). However, phenotypes have been observed in postnatal settings (Paquet-Fifield et al., 2013) and during pathological processes (Stacker et al., 2001). Furthermore, Vegfd genetically interacts with Sox18 during mouse blood vascular development (Duong et al., 2014), suggesting its potential during embryonic development. Our findings are made by high-resolution quantitative analysis of lymphangiogenesis, including determining total LEC numbers per vessel. These phenotypes demonstrate that Vegfd plays compensatory roles with Vegfc in both the face and trunk, and Vegfd alone is indispensable during facial lymphangiogenesis of the LFL and MFL (see Fig. 7). These findings warrant further detailed analysis of LEC number in different vessel beds in the *Vegfc, Vegfd* double-knockout murine model. Of relevance to human lymphatic disease, we show that *vegfd* gene dose broadly modifies Vegfc/Flt4 pathway phenotypes in a variety of mutant models and settings. Zebrafish with mutations in genes involved in this pathway are disease models of heritable lymphedema (Alders et al., 2009; Connell et al., 2010, 2009; Crawford et al., 2016; Evans et al., 2003; Gordon et al., 2013; Hogan et al., 2009a,b; Karkkainen et al., 2000; Shin et al., 2016b; Villefranc et al., 2013). Given that ∼30% of cases of primary (inherited) lymphoedema are caused by mutations in the Ccbe1/Vegfc/Vegfr3 (Flt4) pathway (Mendola et al., 2013), it may be that Vegfd variants can modify patient outcomes.

During primary angiogenesis in zebrafish, *vegfc* and *vegfd* are expressed in the DA and the trunk, respectively (Duong et al., 2014; Hogan et al., 2009b). Despite this, normal angiogenesis was observed in *vegfc*, *vegfd* double mutants and is also seen in *flt4*-null

Development (2017) 144, 507-518 doi:10.1242/dev.146969

mutants (Kok et al., 2015). Both Dll4 and Flt1 negatively regulate arterial angiogenesis, with loss of either resulting in severe hyperbranching of the aISVs (Krueger et al., 2011; Leslie et al., 2007; Siekmann and Lawson, 2007). Here, we find that both Vegfc and Vegfd contribute to these phenotypes (see Fig. 7). Interestingly, although the aISV defects observed upon overexpression of *vegfd* and *vegfc* are grossly similar, the ligands appear to act through different mechanisms. The *vegfc* overexpression phenotype is strongly enhanced in the absence of Dll4, whereas the *vegfd* overexpression phenotype is only slightly enhanced (Hogan et al., 2009b). Consistent with this, we found that the bilateral turning of aISVs following injection of *vegfc* mRNA requires Flt4 and following injection of *vegfd* mRNA requires Kdr. Overall, our data suggest that zebrafish Vegfd can signal through Kdr (Vegfr2) during primary angiogenesis and most likely through Flt4 during secondary angiogenesis based on genetic interactions. Interestingly, a recent study by Shin et al. shows that Prox1 induction in zebrafish facial lymphatics can occur in the absence of Flt4 signaling (Shin et al., 2016b), but in the trunk the induction of Prox1 expression is Vegfc/Flt4 dependent (Koltowska et al., 2015; Shin et al., 2016b). These studies combined suggest that differential signaling events are at play in facial and trunk lymphangiogenesis. Perhaps, given our findings, further examination of Vegfd signaling may help to illuminate these different mechanisms.

Our biochemical data show that Vegfd is capable of binding to Kdr but not to Kdrl. Zebrafish Vegfd is capable of rescuing Vegfaa zebrafish mutants (Rossi et al., 2016), which strongly supports our data and together suggests that Vegfd can activate signaling downstream of Kdr. As mouse Vegfd does not bind to Vegfr2 but the human protein does (Baldwin et al., 2001a), zebrafish may present a very useful alternative model for studying the function of VEGFD/VEGFR2 signaling. Further to these binding studies, we also show that full-length zebrafish Vegfd is processed by proteolytic cleavage of the N- and C-terminal propeptides to generate the mature Vegfd peptide. This resembles the processing of mammalian/human VEGFD, via the proprotein convertases furin, PC5 and PC7 (McColl et al., 2003, 2007), and the processing of zebrafish Vegfc, which likely requires the proprotein convertases furin, PC5 and PC7 (Khatib et al., 2010), similar to requirements in mammalian systems (Joukov et al., 1996; Siegfried et al., 2003). Activation of VEGFC requires CCBE1 and ADAMSTS3, but VEGFD is not processed in a CCBE1-dependent manner in these mammalian models (Bui et al., 2016; Jeltsch et al., 2014). By contrast, in zebrafish-overexpression models it was shown that Vegfd activity is Ccbe1 dependent (Astin et al., 2014). Uncovering differences between species in VEGF processing, activation and signaling may reveal novel and selective capabilities that can be exploited therapeutically and further our fundamental understanding of vascular development.

MATERIALS AND METHODS

Zebrafish

All zebrafish strains were maintained and animal work performed in accordance with the guidelines of the animal ethics committee at The University of Queensland, Australia. The previously published transgenic and mutant lines are listed in Table S1.

TALEN genome editing

Talen monomers (Table S2) for *vegfd* and *dll4* were generated using the golden gate kit (Cermak et al., 2011), cloned into the pCS2TAL3RR and pCS2TAL3DD backbones and transcribed as previously described (Dahlem et al., 2012). Fish were screened by high resolution melt analysis (HRMA) using a Viia7 Real-Time PCR System (Applied Biosystems) and F1 embryos carrying a 7 bp deletion for *vegfd* and 2 bp for *dll4* were outcrossed to *Tg(flt:YFP);Tg(-5.2lyve1b:dsRed)* to generate an F2 population. Primers for HRMA and sequencing of individual mutations are listed in Table S2.

Injections, qPCR and genotyping

Capped RNA was transcribed and injected as previously described (Hogan et al., 2009b). MOs used are listed in Table S3. DNA extraction from fin clips and embryos was performed as previously described (Dahlem et al., 2012). Primers for genotyping *vegfd* and *vegfc* mutants by KASP assays (LGC Genomics) are listed in Table S2. *dll4* mutants were genotyped by *Eco*RI restriction digest of amplified PCR product (Table S2). Quantitative real-time PCR was performed as previously described (Coxam et al., 2014) using the primers indicated in Table S2.

Imaging

Zebrafish embryos were mounted in 0.5% low melting agarose and imaged using a Zeiss LSM 710 FCS confocal microscope. Images were processed using Image J 1.47 software (National Institutes of Health). The number of nuclei expressing *Tg(fli1a:negfp)* and co-expressing *Tg(-5.2lyve1b:dsRed)* in the TD or facial lymphatics were manually counted through a *z*-stack. Nuclei in the MFL and LFL were counted from the branch point of these two vessels. Quantification of bilateral turning of aISVs at 28-32 hpf, hyperbranching of aISVs at 3 dpf and PLs in 54 hpf, and TD in 5 dpf embryos was performed by live scoring using a Leica M165FC microscope.

Expression vectors

The extracellular domains for Kdr (amino acids 23-773) and Kdrl (amino acids 29-738) were PCR amplified and cloned using Infusion enzyme (Clontech, CA, USA) into the pFUSE-mlgG2Aa-Fc2 (IL2ss) vector (InvivoGen, CA, USA) using the primers listed in Table S2. Full-length *vegfd* cDNA encoding both N- and C-terminal propeptides flanking the Vegfd homology domain (VHD) (with the signal peptide amino acids 1-22 removed) and cDNA encoding the zebrafish Vegfd VHD (amino acids 85-198) were PCR amplified using primers listed in Table S2. Products were then cloned into pEFBOSSFLAG (Achen et al., 1998) immediately downstream from the DNA sequence for the interleukin 3 signal sequence using Infusion enzyme (Clontech, CA, USA) to generate zVegf-d-FULL-N-FLAG and zVegf-dΔNΔC-FLAG, respectively. A threonine and an arginine residue were included in the Vegfd constructs as artifacts from cloning, see Fig. 5 for details.

Transient transfections and receptor binding assays

HEK293T cells were maintained in DMEM supplemented with 10% FBS, 2 mM glutamax (Life Technologies Australia, Victoria, Australia), 100 U/ml penicillin and 100 µg/ml streptomycin (Life Technologies Australia) at 37°C in a humidified atmosphere of 10% CO_2.

HEK293T cells were transfected with expression vectors, as indicated, using lipofectamine 2000 (Life Technologies Australia) according to the manufacturer's instructions. Briefly, cells in 5 ml of DMEM in 10 mm tissue culture dishes were transfected with 10 µg of plasmid DNA and 40 µl of lipofectamine 2000. Cells were then incubated for 6 h before addition of 5 ml of DMEM containing 0.4% BSA, and were then starved by further incubation for 24 h. Conditioned media (CM) were collected and clarified via centrifugation at 150 ***g*** for 5 min at room temperature. CM containing Vegfd derivatives were used either directly for western blotting or in binding studies with Ig-fusion proteins. For binding studies, Ig-fusion proteins were precipitated from CM with protein A-sepharose (Sigma Aldrich, MO, USA) by incubation at 4°C for 3 h followed by centrifugation (1500 ***g*** for 5 min at 4°C). Ig-fusion proteins bound to protein A-sepharose were then incubated with CM containing zebrafish Vegfd for 16 h at 4°C, and the sepharose was then washed once with 50 mM Tris-HCl (pH 8.0), 150 mM NaCl, 0.1% Triton X-100, once with 500 mM NaCl and once with 50 mM Tris-HCl (pH 8.0), before heating in reducing LDS sample buffer (Life Technologies Australia) at 95°C for 5 min. Samples were then analyzed by SDS-PAGE/western blotting using Bolt 4-12% Bis Tris plus gels (Invitrogen, CA, USA) and proteins were transferred to iBlot2 nitrocellulose membrane (Invitrogen)

Development (2017) 144, 507-518 doi:10.1242/dev.146969

using an iBlot2 protein transfer apparatus (Life Technologies, CA, USA). Blots were probed with M2 anti-FLAG monoclonal antibody (catalogue number F3165; Sigma-Aldrich) that had been conjugated to 800 IR dye (LI-COR Biosciences, NE, USA) according to the dye manufacturer. Detection was performed using an Odyssey Cx imaging system (LI-COR Biosciences). Soluble Ig-fusion proteins used for binding studies were shown to be of expected sizes by western blotting with goat anti-mouse IgG antibodies (catalogue number 926-32210, LI-COR Biosciences).

Statistical analysis

Statistical analysis was performed using Prism software (GraphPad software). When data conformed to parametric assumptions, ANOVA using Fisher's individual error post-hoc test was used to identify significant differences. When parametric assumptions were not met, Kruskal–Wallis test was used.

Acknowledgements

Imaging was performed in the Australian Cancer Research Foundation's Dynamic Imaging Facility at IMB. We thank Kylie Georgas for help with figures and critical reading of the manuscript.

Competing interests

M.G.A. and S.A.S. are shareholders in Opthea Limited.

Author contributions

N.I.B. designed and performed experiments, and wrote the manuscript. A.J.V., L.L.G. and H.C. contributed to experimental data. S.A.S., M.G.A. and B.M.H. designed experiments and wrote the manuscript.

Funding

This work was supported by the National Health and Medical Research Council of Australia and by a Senior Research Fellowship (1050138, 1053535 and 1042460 to S.A.S.). B.M.H. was supported by a co-funded National Health and Medical Research Council/National Heart Foundation of Australia Career Development Fellowship (100442, 1083811).

Supplementary information

Supplementary information available online at
http://dev.biologists.org/lookup/doi/10.1242/dev.146969.supplemental

References

Achen, M. G., Jeltsch, M., Kukk, E., Makinen, T., Vitali, A., Wilks, A. F., Alitalo, K. and Stacker, S. A. (1998). Vascular endothelial growth factor D (VEGF-D) is a ligand for the tyrosine kinases VEGF receptor 2 (Flk1) and VEGF receptor 3 (Flt4). *Proc. Natl. Acad. Sci. USA* **95**, 548-553.

Achen, M. G., McColl, B. K. and Stacker, S. A. (2005). Focus on lymphangiogenesis in tumor metastasis. *Cancer Cell* **7**, 121-127.

Alders, M., Hogan, B. M., Gjini, E., Salehi, F., Al-Gazali, L., Hennekam, E. A., Holmberg, E. E., Mannens, M. M. A. M., Mulder, M. F., Offerhaus, G. J. A. et al. (2009). Mutations in CCBE1 cause generalized lymph vessel dysplasia in humans. *Nat. Genet.* **41**, 1272-1274.

Astin, J. W., Haggerty, M. J. L., Okuda, K. S., Le Guen, L., Misa, J. P., Tromp, A., Hogan, B. M., Crosier, K. E. and Crosier, P. S. (2014). Vegfd can compensate for loss of Vegfc in zebrafish facial lymphatic sprouting. *Development* **141**, 2680-2690.

Bahary, N., Goishi, K., Stuckenholz, C., Weber, G., LeBlanc, J., Schafer, C. A., Berman, S. S., Klagsbrun, M. and Zon, L. I. (2007). Duplicate VegfA genes and orthologues of the KDR receptor tyrosine kinase family mediate vascular development in the zebrafish. *Blood* **110**, 3627-3636.

Baldwin, M. E., Catimel, B., Nice, E. C., Roufail, S., Hall, N. E., Stenvers, K. L., Karkkainen, M. J., Alitalo, K., Stacker, S. A. and Achen, M. G. (2001a). The specificity of receptor binding by vascular endothelial growth factor-d is different in mouse and man. *J. Biol. Chem.* **276**, 19166-19171.

Baldwin, M. E., Roufail, S., Halford, M. M., Alitalo, K., Stacker, S. A. and Achen, M. G. (2001b). Multiple forms of mouse vascular endothelial growth factor-D are generated by RNA splicing and proteolysis. *J. Biol. Chem.* **276**, 44307-44314.

Baldwin, M. E., Halford, M. M., Roufail, S., Williams, R. A., Hibbs, M. L., Grail, D., Kubo, H., Stacker, S. A. and Achen, M. G. (2005). Vascular endothelial growth factor D is dispensable for development of the lymphatic system. *Mol. Cell. Biol.* **25**, 2441-2449.

Bui, H. M., Enis, D., Robciuc, M. R., Nurmi, H. J., Cohen, J., Chen, M., Yang, Y., Dhillon, V., Johnson, K., Zhang, H. et al. (2016). Proteolytic activation defines distinct lymphangiogenic mechanisms for VEGFC and VEGFD. *J. Clin. Invest.* **126**, 2167-2180.

Bussmann, J., Lawson, N., Zon, L. and Schulte-Merker, S. and **Zebrafish Nomenclature Committee** (2008). Zebrafish VEGF receptors: a guideline to nomenclature. *PLoS Genet.* **4**, e1000064.

Cermak, T., Doyle, E. L., Christian, M., Wang, L., Zhang, Y., Schmidt, C., Baller, J. A., Somia, N. V., Bogdanove, A. J. and Voytas, D. F. (2011). Efficient design and assembly of custom TALEN and other TAL effector-based constructs for DNA targeting. *Nucleic Acids Res.* **39**, e82.

Cha, Y. R., Fujita, M., Butler, M., Isogai, S., Kochhan, E., Siekmann, A. F. and Weinstein, B. M. (2012). Chemokine signaling directs trunk lymphatic network formation along the preexisting blood vasculature. *Dev. Cell* **22**, 824-836.

Connell, F. C., Ostergaard, P., Carver, C., Brice, G., Williams, N., Mansour, S., Mortimer, P. S. and Jeffery, S. (2009). Analysis of the coding regions of VEGFR3 and VEGFC in Milroy disease and other primary lymphoedemas. *Hum. Genet.* **124**, 625-631.

Connell, F., Kalidas, K., Ostergaard, P., Brice, G., Homfray, T., Roberts, L., Bunyan, D. J., Mitton, S., Mansour, S., Mortimer, P. et al. (2010). Linkage and sequence analysis indicate that CCBE1 is mutated in recessively inherited generalised lymphatic dysplasia. *Hum. Genet.* **127**, 231-241.

Covassin, L. D., Villefranc, J. A., Kacergis, M. C., Weinstein, B. M. and Lawson, N. D. (2006). Distinct genetic interactions between multiple Vegf receptors are required for development of different blood vessel types in zebrafish. *Proc. Natl. Acad. Sci. USA* **103**, 6554-6559.

Coxam, B., Sabine, A., Bower, N. I., Smith, K. A., Pichol-Thievend, C., Skoczylas, R., Astin, J. W., Frampton, E., Jaquet, M., Crosier, P. S. et al. (2014). Pkd1 regulates lymphatic vascular morphogenesis during development. *Cell Rep.* **7**, 623-633.

Crawford, J., Bower, N. I., Hogan, B. M., Taft, R. J., Gabbett, M. T., McGaughran, J. and Simons, C. (2016). Expanding the genotypic spectrum of CCBE1 mutations in Hennekam syndrome. *Am. J. Med. Genet. A* **170**, 2694-2697.

Dahlem, T. J., Hoshijima, K., Jurynec, M. J., Gunther, D., Starker, C. G., Locke, A. S., Weis, A. M., Voytas, D. F. and Grunwald, D. J. (2012). Simple methods for generating and detecting locus-specific mutations induced with TALENs in the zebrafish genome. *PLoS Genet.* **8**, e1002861.

Duong, T., Koltowska, K., Pichol-Thievend, C., Le Guen, L., Fontaine, F., Smith, K. A., Truong, V., Skoczylas, R., Stacker, S. A., Achen, M. G. et al. (2014). VEGFD regulates blood vascular development by modulating SOX18 activity. *Blood* **123**, 1102-1112.

Evans, A. L., Bell, R., Brice, G., Comeglio, P., Lipede, C., Jeffery, S., Mortimer, P., Sarfarazi, M. and Child, A. H. (2003). Identification of eight novel VEGFR-3 mutations in families with primary congenital lymphoedema. *J. Med. Genet.* **40**, 697-703.

Gordon, K., Schulte, D., Brice, G., Simpson, M. A., Roukens, M. G., van Impel, A., Connell, F., Kalidas, K., Jeffery, S., Mortimer, P. S. et al. (2013). Mutation in vascular endothelial growth factor-C, a ligand for vascular endothelial growth factor receptor-3, is associated with autosomal dominant milroy-like primary lymphedema. *Circ. Res.* **112**, 956-960.

Gore, A. V., Swift, M. R., Cha, Y. R., Lo, B., McKinney, M. C., Li, W., Castranova, D., Davis, A., Mukouyama, Y.-s. and Weinstein, B. M. (2011). Rspo1/Wnt signaling promotes angiogenesis via Vegfc/Vegfr3. *Development* **138**, 4875-4886.

Haiko, P., Makinen, T., Keskitalo, S., Taipale, J., Karkkainen, M. J., Baldwin, M. E., Stacker, S. A., Achen, M. G. and Alitalo, K. (2008). Deletion of vascular endothelial growth factor C (VEGF-C) and VEGF-D is not equivalent to VEGF receptor 3 deletion in mouse embryos. *Mol. Cell. Biol.* **28**, 4843-4850.

Harris, N. C., Paavonen, K., Davydova, N., Roufail, S., Sato, T., Zhang, Y.-F., Karnezis, T., Stacker, S. A. and Achen, M. G. (2011). Proteolytic processing of vascular endothelial growth factor-D is essential for its capacity to promote the growth and spread of cancer. *FASEB J.* **25**, 2615-2625.

Hiratsuka, S., Minowa, O., Kuno, J., Noda, T. and Shibuya, M. (1998). Flt-1 lacking the tyrosine kinase domain is sufficient for normal development and angiogenesis in mice. *Proc. Natl. Acad. Sci. USA* **95**, 9349-9354.

Hogan, B. M., Bos, F. L., Bussmann, J., Witte, M., Chi, N. C., Duckers, H. J. and Schulte-Merker, S. (2009a). Ccbe1 is required for embryonic lymphangiogenesis and venous sprouting. *Nat. Genet.* **41**, 396-398.

Hogan, B. M., Herpers, R., Witte, M., Helotera, H., Alitalo, K., Duckers, H. J. and Schulte-Merker, S. (2009b). Vegfc/Flt4 signalling is suppressed by Dll4 in developing zebrafish intersegmental arteries. *Development* **136**, 4001-4009.

Isogai, S., Lawson, N. D., Torrealday, S., Horiguchi, M. and Weinstein, B. M. (2003). Angiogenic network formation in the developing vertebrate trunk. *Development* **130**, 5281-5290.

Jakobsson, L., Franco, C. A., Bentley, K., Collins, R. T., Ponsioen, B., Aspalter, I. M., Rosewell, I., Busse, M., Thurston, G., Medvinsky, A. et al. (2010). Endothelial cells dynamically compete for the tip cell position during angiogenic sprouting. *Nat. Cell Biol.* **12**, 943-953.

Jeltsch, M., Jha, S. K., Tvorogov, D., Anisimov, A., Leppanen, V.-M., Holopainen, T., Kivela, R., Ortega, S., Karpanen, T. and Alitalo, K. (2014). CCBE1 enhances lymphangiogenesis via A disintegrin and metalloprotease with thrombospondin motifs-3-mediated vascular endothelial growth factor-C activation. *Circulation* **129**, 1962-1971.

Joukov, V., Pajusola, K., Kaipainen, A., Chilov, D., Lahtinen, I., Kukk, E., Saksela, O., Kalkkinen, N. and Alitalo, K. (1996). A novel vascular endothelial growth factor, VEGF-C, is a ligand for the Flt4 (VEGFR-3) and KDR (VEGFR-2) receptor tyrosine kinases. *EMBO J.* **15**, 290-298.

Karkkainen, M. J., Ferrell, R. E., Lawrence, E. C., Kimak, M. A., Levinson, K. L., McTigue, M. A., Alitalo, K. and Finegold, D. N. (2000). Missense mutations interfere with VEGFR-3 signalling in primary lymphoedema. *Nat. Genet.* **25**, 153-159.

Karnezis, T., Shayan, R., Caesar, C., Roufail, S., Harris, N. C., Ardipradja, K., Zhang, Y. F., Williams, S. P., Farnsworth, R. H., Chai, M. G. et al. (2012). VEGF-D promotes tumor metastasis by regulating prostaglandins produced by the collecting lymphatic endothelium. *Cancer Cell* **21**, 181-195.

Khatib, A.-M., Lahlil, R., Scamuffa, N., Akimenko, M.-A., Ernest, S., Lomri, A., Lalou, C., Seidah, N. G., Villoutreix, B. O., Calvo, F., et al. (2010). Zebrafish ProVEGF-C expression, proteolytic processing and inhibitory effect of unprocessed ProVEGF-C during fin regeneration. *PLoS ONE* **5**, e11438.

Kok, F. O., Shin, M., Ni, C.-W., Gupta, A., Grosse, A. S., van Impel, A., Kirchmaier, B. C., Peterson-Maduro, J., Kourkoulis, G., Male, I. et al. (2015). Reverse genetic screening reveals poor correlation between morpholino-induced and mutant phenotypes in zebrafish. *Dev. Cell* **32**, 97-108.

Koltowska, K., Betterman, K. L., Harvey, N. L. and Hogan, B. M. (2013). Getting out and about: the emergence and morphogenesis of the vertebrate lymphatic vasculature. *Development* **140**, 1857-1870.

Koltowska, K., Lagendijk, A. K., Pichol-Thievend, C., Fischer, J. C., Francois, M., Ober, E. A., Yap, A. S. and Hogan, B. M. (2015). Vegfc regulates bipotential precursor division and Prox1 expression to promote lymphatic identity in zebrafish. *Cell Rep.* **13**, 1828-1841.

Krueger, J., Liu, D., Scholz, K., Zimmer, A., Shi, Y., Klein, C., Siekmann, A., Schulte-Merker, S., Cudmore, M., Ahmed, A. et al. (2011). Flt1 acts as a negative regulator of tip cell formation and branching morphogenesis in the zebrafish embryo. *Development* **138**, 2111-2120.

Küchler, A. M., Gjini, E., Peterson-Maduro, J., Cancilla, B., Wolburg, H. and Schulte-Merker, S. (2006). Development of the zebrafish lymphatic system requires VEGFC signaling. *Curr. Biol.* **16**, 1244-1248.

Lawson, N. D. and Weinstein, B. M. (2002). Arteries and veins: making a difference with zebrafish. *Nat. Rev. Genet.* **3**, 674-682.

Lawson, N. D., Vogel, A. M. and Weinstein, B. M. (2002). sonic hedgehog and vascular endothelial growth factor act upstream of the Notch pathway during arterial endothelial differentiation. *Dev. Cell* **3**, 127-136.

Le Guen, L., Karpanen, T., Schulte, D., Harris, N. C., Koltowska, K., Roukens, G., Bower, N. I., van Impel, A., Stacker, S. A., Achen, M. G. et al. (2014). Ccbe1 regulates Vegfc-mediated induction of Vegfr3 signaling during embryonic lymphangiogenesis. *Development* **141**, 1239-1249.

Leslie, J. D., Ariza-McNaughton, L., Bermange, A. L., McAdow, R., Johnson, S. L. and Lewis, J. (2007). Endothelial signalling by the Notch ligand Delta-like 4 restricts angiogenesis. *Development* **134**, 839-844.

McColl, B. K., Baldwin, M. E., Roufail, S., Freeman, C., Moritz, R. L., Simpson, R. J., Alitalo, K., Stacker, S. A. and Achen, M. G. (2003). Plasmin activates the lymphangiogenic growth factors VEGF-C and VEGF-D. *J. Exp. Med.* **198**, 863-868.

McColl, B. K., Paavonen, K., Karnezis, T., Harris, N. C., Davydova, N., Rothacker, J., Nice, E. C., Harder, K. W., Roufail, S., Hibbs, M. L. et al. (2007). Proprotein convertases promote processing of VEGF-D, a critical step for binding the angiogenic receptor VEGFR-2. *FASEB J.* **21**, 1088-1098.

Mendola, A., Schlögel, M. J., Ghalamkarpour, A., Irrthum, A., Nguyen, H. L., Fastré, E., Bygum, A., van der Vleuten, C., Fagerberg, C., Baselga, E. et al. (2013). Mutations in the VEGFR3 signaling pathway explain 36% of familial lymphedema. *Mol. Syndromol.* **4**, 257-266.

Nasevicius, A., Larson, J. and Ekker, S. C. (2000). Distinct requirements for zebrafish angiogenesis revealed by a VEGF-A morphant. *Yeast* **17**, 294-301.

Okuda, K. S., Astin, J. W., Misa, J. P., Flores, M. V., Crosier, K. E. and Crosier, P. S. (2012). lyve1 expression reveals novel lymphatic vessels and new mechanisms for lymphatic vessel development in zebrafish. *Development* **139**, 2381-2391.

Olsson, A.-K., Dimberg, A., Kreuger, J. and Claesson-Welsh, L. (2006). VEGF receptor signalling — in control of vascular function. *Nat. Rev. Mol. Cell Biol.* **7**, 359-371.

Paquet-Fifield, S., Levy, S. M. Sato, T., Shayan, R., Karnezis, T., Davydova, N., Nowell, C. J., Roufail, S., Ma, G. Z.-M., Zhang, Y.-F., et al. (2013). Vascular endothelial growth factor-d modulates caliber and function of initial lymphatics in the dermis. *J. Invest. Dermatol.* **133**, 2074-2084.

Rissanen, T. T., Markkanen, J. E., Gruchala, M., Heikura, T., Puranen, A., Kettunen, M. I., Kholová, I., Kauppinen, R. A., Achen, M. G., Stacker, S. A. et al. (2003). VEGF-D is the strongest angiogenic and lymphangiogenic effector among VEGFs delivered into skeletal muscle via adenoviruses. *Circ. Res.* **92**, 1098-1106.

Rossi, A., Gauvrit, S., Marass, M., Pan, L., Moens, C. B. and Stainier, D. Y. (2016). Regulation of Vegf signaling by natural and synthetic ligands. *Blood* **128**, 2359-2366.

Shin, M., Beane, T., Quillien, A., Male, I., Zhu, L. J. and Lawson, N. D. (2016a). Vegfa signals through ERK to promote angiogenesis, but not artery differentiation. *Development* **143**, 3796-3805.

Shin, M., Male, I., Beane, T. J., Villefranc, J. A., Kok, F. O., Zhu, L. J. and Lawson, N. D. (2016b). Vegfc acts through ERK to induce sprouting and differentiation of trunk lymphatic progenitors. *Development* **143**, 3785-3795.

Siegfried, G., Basak, A., Cromlish, J. A., Benjannet, S., Marcinkiewicz, J., Chrétien, M., Seidah, N. G. and Khatib, A.-M. (2003). The secretory proprotein convertases furin, PC5, and PC7 activate VEGF-C to induce tumorigenesis. *J. Clin. Investig.* **111**, 1723-1732.

Siekmann, A. F. and Lawson, N. D. (2007). Notch signalling limits angiogenic cell behaviour in developing zebrafish arteries. *Nature* **445**, 781-784.

Stacker, S. A., Stenvers, K., Caesar, C., Vitali, A., Domagala, T., Nice, E., Roufail, S., Simpson, R. J., Moritz, R., Karpanen, T. et al. (1999). Biosynthesis of vascular endothelial growth factor-D involves proteolytic processing which generates non-covalent homodimers. *J. Biol. Chem.* **274**, 32127-32136.

Stacker, S. A., Caesar, C., Baldwin, M. E., Thornton, G. E., Williams, R. A., Prevo, R., Jackson, D. G., Nishikawa, S., Kubo, H. and Achen, M. G. (2001). VEGF-D promotes the metastatic spread of tumor cells via the lymphatics. *Nat. Med.* **7**, 186-191.

Stacker, S. A., Achen, M. G., Jussila, L., Baldwin, M. E. and Alitalo, K. (2002). Metastasis: Lymphangiogenesis and cancer metastasis. *Nat. Rev. Cancer* **2**, 573-583.

Stacker, S. A., Williams, S. P., Karnezis, T., Shayan, R., Fox, S. B. and Achen, M. G. (2014). Lymphangiogenesis and lymphatic vessel remodelling in cancer. *Nat. Rev. Cancer* **14**, 159-172.

Villefranc, J. A., Nicoli, S., Bentley, K., Jeltsch, M., Zarkada, G., Moore, J. C., Gerhardt, H., Alitalo, K. and Lawson, N. D. (2013). A truncation allele in vascular endothelial growth factor c reveals distinct modes of signaling during lymphatic and vascular development. *Development* **140**, 1497-1506.

Von Marschall, Z., Scholz, A., Stacker, S. A., Achen, M. G., Jackson, D. G., Alves, F., Schirner, M., Haberey, M., Thierauch, K. H., Wiedenmann, B. et al. (2005). Vascular endothelial growth factor-D induces lymphangiogenesis and lymphatic metastasis in models of ductal pancreatic cancer. *Int. J. Oncol.* **27**, 669-679.

Wiley, D. M., Kim, J.-D., Hao, J., Hong, C. C., Bautch, V. L. and Jin, S.-W. (2011). Distinct signalling pathways regulate sprouting angiogenesis from the dorsal aorta and the axial vein. *Nat. Cell Biol.* **13**, 686-692.

Yaniv, K., Isogai, S., Castranova, D., Dye, L., Hitomi, J. and Weinstein, B. M. (2006). Live imaging of lymphatic development in the zebrafish. *Nat. Med.* **12**, 711-716.